TSPO PET imaging of natalizumab-associated progressive multifocal leukoencephalopathy

Mahler, Christoph; Schumacher, Adrian-Minh; Unterrainer, Marcus; Kaiser, Lena; Höllbacher, Thomas; Lindner, Simon; Havla, Joachim; Ertl-Wagner, Birgit; Patzig, Maximilian; Seelos, Klaus; Neitzel, Julia; Mäurer, Matthias; Krumbholz, Markus; Metz, Imke [**and 9 more**]

How to cite

MAHLER, Christoph et al. TSPO PET imaging of natalizumab-associated progressive multifocal leukoencephalopathy. In: Brain, 2021. doi: 10.1093/brain/awab127

This publication URL: https://archive-ouverte.unige.ch/unige:151695

Publication DOI: 10.1093/brain/awab127

TSPO PET imaging of natalizumab-associated progressive multifocal leukoencephalopathy

Christoph Mahler,[1,2,†] Adrian-Minh Schumacher,[1,2,†] Marcus Unterrainer,[3] Lena Kaiser,[3] Thomas Höllbacher,[3] Simon Lindner,[3] Joachim Havla,[1,2] Birgit Ertl-Wagner,[4] Maximilian Patzig,[5] Klaus Seelos,[5] Julia Neitzel,[6] Matthias Mäurer,[7] Markus Krumbholz,[8] Imke Metz,[9] Wolfgang Brück,[9] Christine Stadelmann,[9] Doron Merkler,[10,11] Achim Gass,[12] Vladimir Milenkovic,[13] Peter Bartenstein,[3,14] Nathalie L. Albert,[3] Tania Kümpfel[1,2,‡] and Martin Kerschensteiner[1,2,14,‡]

[†,‡]**These authors contributed equally to this work.**

Abstract

Progressive multifocal leukoencephalopathy (PML) is a severe infection of the central nervous system caused by the polyomavirus JC (JCV) that can occur in multiple sclerosis (MS) patients treated with natalizumab. Clinical management of patients with natalizumab-associated PML is challenging not the least because current imaging tools for the early detection, longitudinal monitoring and differential diagnosis of PML lesions are limited. Here we evaluate whether TSPO positron emission tomography (PET) imaging can be applied to monitor the inflammatory activity of PML lesions over time and differentiate them from MS lesions. For this monocenter pilot study we followed 8 patients with natalizumab-associated PML with PET imaging using the TSPO radioligand [^{18}F]GE-180 combined with frequent 3T MRI imaging. In addition we compared TSPO PET signals in PML lesions with the signal pattern of MS lesions from 17 independent MS patients. We evaluated the standardized uptake value ratio (SUVR) as well as the morphometry of the TSPO uptake for putative PML and MS lesions areas compared to a radiologically unaffected pseudo-reference region in the cerebrum. Furthermore TSPO expression in situ was immunohistochemically verified by determining the density and cellular identity of TSPO-expressing cells in brain sections from four patients with early natalizumab-associated PML as well as five patients with other forms of PML and six patients with inflammatory demyelinating CNS lesions (clinically isolated syndrome/MS). Histological analysis revealed a reticular accumulation of TSPO expressing phagocytes in PML lesions, while such phagocytes showed a more homogenous distribution in putative MS lesions. TSPO PET imaging showed an enhanced tracer uptake in natalizumab-associated PML lesions that was present from the early to the chronic stages (up to 52 months after PML diagnosis). While

gadolinium enhancement on MRI rapidly declined to baseline levels, TSPO tracer uptake followed a slow one phase decay curve. A TSPO-based 3-dimensional diagnostic matrix taking into account the uptake levels as well as the shape and texture of the TSPO signal differentiated more than 96% of PML and MS lesions. Indeed, treatment with rituximab after natalizumab-associated PML in three patients did not affect tracer uptake in the assigned PML lesions but reverted tracer uptake to baseline in the assigned active MS lesions. Taken together our study suggests that TSPO PET imaging can reveal CNS inflammation in natalizumab-associated PML. TSPO PET may facilitate longitudinal monitoring of disease activity and help to distinguish recurrent MS activity from PML progression.

Author affiliations:

1 Institute of Clinical Neuroimmunology, University Hospital, Ludwig-Maximilians-Universität Munich, Munich, Germany

2 Biomedical Center (BMC), Medical Faculty, Ludwig-Maximilians-Universität Munich, Martinsried, Germany

3 Department of Nuclear Medicine, University Hospital, Ludwig-Maximilians-Universität Munich, Munich, Germany

4 Institute of Clinical Radiology, University Hospital Ludwig-Maximilians-Universität Munich, Munich, Germany

5 Institute of Neuroradiology, University Hospital, Ludwig-Maximilians-Universität Munich, Munich, Germany

6 Institute for Stroke and Dementia Research, Ludwig-Maximilians-Universität Munich, Munich, Germany

7 Department of Neurology, Juliusspital, Würzburg, Germany

8 Department of Neurology & Stroke and Hertie-Institute for Clinical Brain Research, Eberhard Karl University of Tübingen, Tübingen, Germany

9 Institute of Neuropathology, University Medical Center Göttingen, Göttingen, Germany

10 Division of Clinical Pathology, Geneva University Hospital, Geneva, Switzerland

11 Department of Pathology and Immunology, University of Geneva, Geneva, Switzerland

12 Department of Neurology, University Hospital Mannheim, Mannheim, Germany

13 Department of Psychiatry and Psychotherapy, University of Regensburg, Regensburg, Germany

14 Munich Cluster of Systems Neurology (SyNergy), Munich, Germany

Correspondence to: Tania Kümpfel

Institute of Clinical Neuroimmunology

LMU Klinikum

Marchioninistr. 15

81377 Munich, Germany
E-mail: tania.kümpfel@med.uni-muenchen.de

Correspondence may also be addressed to: Martin Kerschensteiner
E-mail: martin.kerschensteiner@med.uni-muenchen.de

Running title: TSPO PET imaging of natalizumab-associated PML

Keywords: progressive multifocal leukoencephalopathy; multiple sclerosis; positron emission tomography; translocator protein; microglia

Introduction

In recent years an increasing number of progressive multifocal leukoencephalopathy (PML) cases – a severe opportunistic infection of the central nervous system (CNS) caused by polyomavirus JC (JCV) – have been observed as a complication of multiple sclerosis (MS) therapy with natalizumab [1]. While natalizumab-associated PML per se is a rare complication with an estimated incidence of about 3.99/1,000 patients as of March 2020 [2], natalizumab is widely used in MS therapy and as a result, more than 832 cases have now been confirmed across the globe [2]. Clinical management of patients with natalizumab-associated PML has remained challenging with a fatality rate of the disease of more than 20 % and varying levels of disability in those who survive [2,3]. Management of surviving patients is further complicated by immune reconstitution inflammatory syndrome (IRIS) and the re-occurrence of MS-related disease activity at variable time points after cessation of natalizumab therapy [4-6]. Tools that allow specific monitoring of PML activity are thus of critical importance for clinical management.

Magnetic resonance imaging (MRI) can reveal tissue alterations caused by PML and is the current gold standard for brain imaging of PML patients [7]. While MRI has proven to be a valuable tool for clinical diagnosis and management of these patients, important aspects such as the early detection and the long-term monitoring of PML activity as well as the unequivocal differentiation of MS and PML related inflammatory activity have remained challenging [8]. One approach to meet these challenges can be positron emission tomography (PET) imaging of radioligands that bind to the mitochondrial 18 kDa translocator protein (TSPO) [9]. TSPO PET is based on the observation that mononuclear phagocytes upregulate the expression of the TSPO protein upon activation [10,11] and has been used to measure CNS inflammation in multiple sclerosis [12-15] and other neurological conditions [16,17]. This is relevant in the context of natalizumab-associated PML as previous histological analyses showed that mononuclear phagocytes (either locally activated microglial cells or invading monocyte-derived macrophages) are important contributors to the inflammatory reaction in this disease [18,19]. Here we use the TSPO radioligand [^{18}F]GE-180 that has been shown to detect CNS inflammation in MS and glioma patients and is also susceptible to changes in blood-brain barrier permeability [20-22]. For this purpose we first verified that TSPO-expressing mononuclear phagocytes accumulate in brain lesions of patients with natalizumab-associated PML and subsequently explored whether TSPO PET can be used for longitudinal monitoring of inflammatory activity in natalizumab-associated PML and differentiation of PML progression from re-occurrence of MS disease activity.

Materials and methods

Tissue Specimens and Histopathological Analysis

For histopathological analysis brain specimens obtained from autopsies and biopsies of patients with natalizumab-associated PML (n=4, **Table 1**), other forms of PML (n=5) or clinically isolated syndrome (CIS)/MS (n=6) were included. Non-MS PML patients (mean age 31.7 ± 2.9 years, information not available for two samples) included two cases of HIV/AIDS-associated PML. CIS/MS patients consisted of two males and four females (mean age 38.2 ± 15.8 years) and showed a disease duration smaller than six months for five of the cases. Brain sections from autopsies (n=4) of patients who died from non-neurological diseases served as controls (two females and two males, mean age 40.8 ± 7 years). Their use for scientific purposes was in accordance with institutional ethical guidelines and was approved by the ethics

committee of the University of Göttingen (Germany) and the University of Geneva (Switzerland).

Immunostaining for TSPO (PBR), mononuclear phagocytes (CD68) and activated astrocytes (GFAP) was carried out on 3-µm thin sections of paraffin-embedded tissue blocks using the following primary and secondary antibodies: monoclonal rabbit anti PBR (1:100, Abcam, #ab109497), monoclonal mouse anti-CD68 (1:100, Dako, M0876) and a chicken polyclonal antibody to GFAP (1:100, Abcam, #ab4674). For quantitative analysis, three regions of interest from each area (PML lesion, PML adjacent white matter, PML adjacent grey matter, actively demyelinating MS lesion) as well as from white matter regions in non-inflammatory control samples were chosen using Pannoramic viewer software (3D-Histech) and quantified using the ImageJ "Cell Counter" plugin.

Study Cohort

In this pilot study we prospectively included MS patients with a diagnosis of natalizumab-associated PML. The local Ethics Committee (IRB no. 48-15) and the German Radiation Protection Committee authorized the study (BfS no. Z 5-22463/2–2015-006). Written informed consent was given by all patients before participation in the study. The following inclusion criteria were applied: age between 18 and 85 years, a diagnosis of MS based on the 2010 revision to the McDonald criteria, and a diagnosis of PML based on the 2013 PML diagnostic criteria [23]. All patients presented with clinical worsening and tested positive for JCV DNA in the CSF. Exclusion criteria were: major psychiatric and/or medical disease, pregnancy, unrelated exposure to >15 mSv per year, and general contraindications to PET/MRI. A total of eight patients with natalizumab-associated PML and RRMS were included (for clinical characteristics see **Table 2** and **Supplementary Fig. 1**). The TSPO binding affinity status was analysed based on polymorphism genotyping at the Department of Psychiatry of the University Hospital Regensburg. For this purpose genomic DNA was extracted from 4 ml of whole blood with QIAamp DNA blood maxi kit (Qiagen, Hilden, Germany) according to the manufacturer's protocol. DNA quality was assessed utilizing optical absorbance and gel electrophoresis. In line with previous studies using the [18F]GE-180 tracer [20,24] we could detect increased tracer uptake in patients with different TSPO binding affinity statuses. Our study included one low-affinity binder (patient #1, mean PML lesional SUVR 1.60), and one medium-affinity binder (patient #7, mean PML lesional SUVR 1.65±0.20), while all remaining patients were high-affinity binders (mean PML lesional SUVR 2.11±0.58).

MRI

MRI was acquired on a Magnetom Skyra 3T scanner (Siemens Healthineers, Erlangen, Germany) with a slice thickness of 3 mm at the Institute of Clinical Radiology, LMU using protocol defined sequences (axial T2-weighted (T2w) and T2-FLAIR, T1-weighted (T1w) including contrast enhanced T1w images). The mean interval between the PET and the correlated MRI scan was 2.9 ± 3.3 days. Serial MRI were complemented by external MRI scans, including standard sequences (T1w, T2w, T2-FLAIR and DWI). PML lesions and MS lesions of all available MRI's (analysing all sequences, including DWI, FLAIR and contrast enhanced MRI) were evaluated by two experienced neuroradiologists (A.G. and M.P) and accordingly classified as PML or MS lesions using standard diagnostic criteria [25,26]. Information on the MRI presentation of MS lesions (number of lesions, lesion location and number of lesions with contrast enhancement) at the timepoint of PET imaging in PML patients is given in **Supplementary Table 1**. PML lesions from the serial MRI evaluations were assigned to the following stages taking into account previously suggested MRI criteria [1]: early symptomatic PML before IRIS (increasing lesion size, little or no gadolinium enhancement), IRIS phase (gadolinium enhancement common, punctate pattern and T1 bright cortical line), post IRIS phase of PML (no gadolinium enhancement, no MRI features of IRIS, but close temporal proximity, ongoing inflammatory activity and tissue repair), post PML (stable phase of persistent tissue defect with atrophy in PML region) as shown in **Supplementary Figure 1**.

MRI contrast analysis

For the quantification of contrast enhancement in MRI within the PET lesion area both the non-contrast-enhanced (NCE-) T1w image and the PET-based volumes of interest (VOI, see below) were co-registered to each patient's contrast-enhanced (CE-) T1w image. The NCE-T1w images were automatically segmented with FreeSurfer (v6.0; http://surfer.nmr.mgh.harvard.edu/) in order to create patient-specific, binary masks of the whole-brain white matter and the lateral ventricles. For patient #4, manual segmentation was applied. To enable quantitative comparisons of signal intensities between the CE-T1w and NCE- images, the signal of each voxel was normalized to the mean signal intensity within the ventricle mask and a contrast ratio score was computed. We defined a ratio score of >1.2 to be contrast positive, with this threshold yielding the strongest signal-to-noise separation. Representative images with overlayed co-registered masks (PET-based VOI, above threshold volume) of two patients with contrast enhancing PML lesions are shown in **Supplementary Figure 3.**

[^{18}F]GE-180 Synthesis

[^{18}F]GE-180 was produced on a FASTlabTM synthesizer with single-use disposable cassettes provided by GE Healthcare (Amstersham, UK). The obtained radiochemical purity was ≥95%. Full GMP requirements for tracer synthesis were met. Detailed specifications were published before [27].

PET acquisition

A Biograph 64 PET/CT scanner (Siemens Healthineers, Erlangen, Germany) at the Department of Nuclear Medicine, LMU was used to scan patients. A low-dose CT scan was acquired for attenuation correction. After i.v. bolus injection of 189±12 MBq [^{18}F]GE-180, emission scans were recorded over 90 minutes in list-mode. Subsequently, an OSEM2D algorithm was applied for image reconstruction (8 iterations, 4 subsets, 4 mm Gauss) with a matrix size of 256 x 256 x 109 and a voxel size of 1.336 x 1.336 x 2.027 mm^3. The transaxial resolution (FWHM at 10cm radial distance and with HI-REZ Option) was 4.8 mm and axial resolution (FWHM at 10cm radial distance and with HI-REZ Option) was 5.4 mm. For scatter, decay, attenuation, and random counts standard corrections were applied.

PET image evaluation

The PMOD Neuro tool was used for evaluation of the PET data based on 60-90 minutes summation images after correction of subject motion and co-registration of PET images on T1w as well as T2/FLAIR MR images. For anatomical VOI definition in PET space, the default

processing workflow within PMOD Neuro tool was applied, utilizing T1w MRI data and the N30R83. Afterwards, each T1w MRI sequence was normalized to MNI space and subsequently a maximum probability atlas [28,29] was applied. VOIs were then transformed into PET space. An established threshold-based method for the segmentation of focal MS lesions [30,20], was adapted for the delineation of both PML lesions and MS lesions in this study. Therefore, a pseudo-reference region (PRR) within the contralateral cortex was chosen as background volume for segmentation. The same pseudo-reference region was used for PML and MS lesions within each patient. A total of 89 MS lesions from 17 (non-PML) MS patients used to train the diagnostic matrix were taken from [20] and delineated as described there. The mean SUV of the PRR was similar for both studies (mean SUV±SD of the PRR in this study: 0.38±0.03 vs. mean SUV±SD of the PRR in [20]: 0.36±0.03). To better understand the temporal reliability of lesion analysis in sequential scans we further analysed the SUV of the PRR in individual patients over time and observed minimal variation of tracer uptake values in the PRR in consecutive scans (**Supplementary Figure 2**).

For quantitative analysis of tracer uptake, the maximum uptake was extracted from a hot-spot comprised of three voxels. The relation of the Gadolinium status and corresponding TSPO tracer uptake (mean SUVR±SD) in individual MS and PML lesions is shown in **Supplementary Table 2**.

Quantitative analysis of TSPO uptake pattern

In order to improve inter- and intra-patient comparability of quantitative values, a normalization to standardized uptake values (SUV = activity concentration × patient weight / injected activity) and SUV-ratios (SUVR = SUV / SUVreference) was performed. From SUVR images first order statistics, texture features, and shape parameters were extracted using an in-house developed software written within the ROOT data analysis framework (version 6.09/01, Cern, Switzerland) integrating algorithms provided within the ITK segmentation and registration toolkit (version 4.11, National Library of Medicine). The following texture features were derived from a grey level co-occurrence matrix: energy, entropy, correlation, inverse difference moment, inertia, cluster shade, cluster prominence, and Haralick's correlation. The included shape parameters were: elongation, roundness, equal sphere radius, flatness, mesh volume and mesh area. For texture analysis, intensity values from SUVR images were discretized using a fixed bin size of 0.05 based on previous studies [31,32]. The cut-off criterion SUVR[Max] was calculated in R (Scatter3D plugin and rgl library (3D Visualization Using OpenGL)) based on the concentration ellipsoid (α) with the level parameter (expected proportion of bivariate-

normal observations) set to 0.95. For matrix analysis lesions were classified as MS-lesions, if they localised outside the PML ellipsoid (green). Respectively, lesions were defined as PML lesions, if they localised outside the MS ellipsoid.

Statistical analysis

Statistical analysis was done with Prism (Versions 6.0 and 7.0, Graphpad) using 1-way ANOVA test (as normal distribution could be assumed), corrected for multiple comparisons using the Turkey or Dunnett's Test. Paired t-test (assuming normal distribution, based on D'Agostino-Pearson test) was applied for statistical analysis of MS and PML lesion before and after anti CD20 therapy.

Data availability

The data that support the findings of this study are available from the corresponding authors, (TK, MK) upon reasonable request.

Results

Histopathological analysis of TSPO expression in acute natalizumab-associated PML

To assess whether TSPO imaging could be a suitable approach to measure inflammatory activity in natalizumab-associated PML, we first characterized the spatial and cellular profile of TSPO immunoreactivity in brain sections from four acute natalizumab-associated PML cases as well as five cases with other forms of PML (non MS PML), six cases of CIS/MS and four age-matched control cases without an inflammatory CNS disease (see **Table 1** and methods section). We observed a marked increase in TSPO immunoreactivity in PML cases that appeared most prominent in the subcortical white matter lesion area and followed a reticular pattern on the macroscale (**Figure 1A**) consistent with the multifocal appearance of PML lesions [23], while TSPO immunoreactivity in active MS lesions appeared more homogenous and was often most pronounced at the lesion border (**Figure 1B**) as previously reported [11]. In natalizumab-associated PML cases the density of TSPO-positive cells was highest within white matter lesions, while the adjacent gray and white matter showed only a moderate increase in relation to control sections (**Figure 1C** and **1D**). To determine the cellular identity of the TSPO-positive cells in PML and MS lesions we counterstained the sections with markers for activated mononuclear phagocytes (CD68) and reactive astrocytes (GFAP) - cell populations that have

been previously shown to express TSPO upon activation [10,33]. Our analysis showed that the (vast) majority of TSPO-positive cells in PML and MS white matter lesions were activated mononuclear phagocytes. While reactive astrocytes were thus only a minor contributor to TSPO expression in the white matter lesions of natalizumab-associated PML, they constituted a sizeable proportion of the TSPO-positive cells in the adjacent white and gray matter. In all investigated areas, only few TSPO-positive cells expressed neither CD68 nor GFAP, indicating that mononuclear phagocytes and astrocytes are the major TSPO-expressing cell types in natalizumab-associated PML (**Figure 1E** and **1F**). Taken together our histological analysis indicate a close spatial correlation of TSPO expression with CNS inflammation in natalizumab-associated PML with the highest density of TSPO-expressing cells in the highly inflammatory white matter lesions. Activated mononuclear phagocytes, either derived from local microglial cells or from infiltrating blood-borne monocytes, are the major cellular source of TSPO expression in these lesions. These results thus provide a rationale for using TSPO PET imaging to track CNS inflammation in patients with natalizumab-associated PML.

Longitudinal monitoring of inflammatory activity in natalizumab-associated PML using [^{18}F] GE180 TSPO PET

To assess whether increased TSPO expression in natalizumab-associated PML can be leveraged for non-invasive monitoring of CNS inflammation we performed TSPO PET imaging in eight MS patients (between 35 and 56 years of age) who developed PML during immunosuppressive therapy with natalizumab (after 46 to 79 infusions; see **Table 2**). PET imaging (n=16 PET scans in eight patients) was performed using the [^{18}F] GE-180 tracer as previously described [20] in parallel to standardized 3T MRI scans and accompanied by frequent additional MRI documentation (**Supplementary Figure 1**). Using this approach, we assessed TSPO tracer uptake in PML lesions at different time points after PML diagnosis and before, during and after clinical and radiological appearance of IRIS. We found that TSPO PET imaging was able to detect PML-associated inflammation at all stages of the disease and even before contrast enhancement indicative of IRIS appeared on MRI scans. This was apparent in patient #3, who was treated with natalizumab for highly active MS and was referred to our hospital with progressive dysarthria and paresis of the left arm three months after the initial diagnosis of PML based on a cortical hyperintense T2/FLAIR lesion in the right precentral gyrus on MRI and the detection of JCV DNA in the CSF. TSPO PET imaging at the time of admission to our hospital (+3) revealed a large area with strongly enhanced tracer uptake in the right fronto-parietal lobe.

This area of enhanced tracer uptake clearly exceeded the corresponding hyperintense signal on T2/FLAIR and isotropic images (DWI) on the corresponding MRI (+3), particularly so towards the parietal region and contrast enhancement on MRI became only visible three weeks later at month 3.5 (**Figure 2**). Likewise on the contralateral (left) side, increased tracer uptake in the absence of altered diffusion restriction could be observed in an area (**Figure 2B**), that only became clearly visible as a T2/FLAIR hyperintense lesion in the follow-up MRI (+3.5). TSPO tracer uptake was still increased at the last documented time point in the post IRIS phase indicating that despite cessation of lesion increase on MRI and cessation of Gd enhancement an increased inflammatory activity persisted in the lesion area.

To further assess whether TSPO PET imaging can also help monitoring inflammatory activity in natalizumab-associated PML over time we measured the mean TSPO SUVR in PML lesions derived from a total of 16 TSPO PET measurements obtained between 0 and 52 months after PML diagnosis. While the extent of the increased tracer uptake in early PML appeared somewhat variable, our results showed that the slowly progressive decline of TSPO tracer uptake following IRIS remarkably closely followed a standard one-phase decay curve and remained elevated for several years after PML diagnosis (**Figure 3A** and **3C**). This is in marked contrast to the temporal evolution of the contrast enhancement measured by MRI in the same lesions that was only detectable during the comparably short IRIS phase of the disease process (**Figure 3A, 3B** and **Supplementary Figure 3**). These findings thus indicate that TSPO PET imaging might be suitable for long term monitoring of PML-associated inflammatory activity that extends substantially beyond the PML-IRIS phase. Moreover, the remarkable consistency of the individual measurements with an interpolated decay curve suggests that the inflammatory activity in PML lesions declines in a rather stereotypic and thus predictable manner over time.

A TSPO-based diagnostic matrix differentiates inflammatory activity in natalizumab-associated PML and MS lesions

To explore whether TSPO PET could reveal distinctive features of CNS inflammation we selected differentiation parameters for each dimension of lesion features (uptake level, texture, shape) via univariate analysis for their power to separate MS lesions (n=89 lesions from an independent cohort of 17 MS patients taken from [20]) from natalizumab-associated PML lesions (n=23 PET lesion analyses (VOIs) derived at different timepoints from 13 PML lesion areas from eight patients). In this analysis optimal differentiation yield was obtained for a combination of (i) the TSPO SUVR[Max], as a measure of the maximal tracer uptake, (ii) the

inertia of the lesions texture as a parameter of local signal homogeneity variability (iii) equal sphere radius, the shape factor that quantifies the sphericity of the lesion. When we plotted the TSPO based measurements of these MS and PML lesions, all acquired with the same PET imaging set-up, in a corresponding 3-dimensional matrix, distinct lesion clouds emerged (**Figure 4A**, **4B** and **Supplementary Figure 4**). Using these criteria more than 96% of all PML and MS lesion analyses could be differentiated (21 of 23 PML lesion analyses and 87 of 89 MS lesions; **Figure 4B**). Moreover all lesions with a high SUVR[MAX] (>2.9; **Figure 4C**) could be clearly separated. The latter is of importance as differentiating highly active MS and PML lesions is critical when facing a patient with newly emerging clinical symptoms after the initial PML episode.

We next assessed whether this TSPO-PET imaging could be helpful in the clinical management of MS patients, who show new clinical symptoms and/or new MRI lesions after diagnosis of a natalizumab-associated PML. While the analysis of the mean TSPO SUVR showed no significant differences between lesions groups (**Supplementary Table 2**), the analysis of the TSPO-based diagnostic matrix allowed us to assign 12 out of 13 lesions that occurred after PML diagnosis in four patients (patients #5, #6. #7, and #8) as "MS lesions". These included one lesion of a patient (#5) that formed in the brain stem in the immediate vicinity of a pre-existing PML lesion and two new enhancing lesions in a patient (#8) with long-lasting JCV DNA positivity in the CSF (**Figure 5A and 5B, Supplementary Figure 1**). Based on these results and supporting MRI and CSF analysis we decided to treat three of these patients with an anti-CD20 immunotherapy (rituximab). While TSPO tracer uptake was comparable between PML and the assigned "MS lesions" prior to treatment, on the follow-up scan between 6 and 32 months after initiation of rituximab therapy, TSPO tracer uptake in all 11 putative "MS lesions" of treated patients had returned close to baseline. In contrast uptake in the pre-existing PML lesions remained mostly unchanged, confirming the correct assignment provided by our TSPO–based diagnostic matrix (**Figure 5C**). Taken together our study thus indicates that TSPO imaging reveals characteristic features of CNS inflammation that can be leveraged to identify distinct inflammatory pathologies and differentiate clinical entities.

Discussion

To our knowledge this is the first study assessing TSPO PET imaging as a tool to monitor inflammatory activity in natalizumab-associated PML. We first validated this approach by

histological analysis of brain tissue sections that showed a pronounced increase of TSPO-positive cells in white matter lesions of both natalizumab-associated and other forms of PML. The vast majority of the TSPO-positive cells in the lesion area are activated phagocytes, derived either from locally activated microglia cells or from infiltrating blood-borne monocytes. This observation is in accordance with a number of previous studies of TSPO expression in other neuroinflammatory conditions [34,11,35,36] and supports the notion that TSPO PET can be used to monitor phagocyte activation in PML lesions.

In line with the marked accumulation of TSPO-positive cells in early PML lesions we observed a robust increase in tracer uptake in early PML lesions. Interestingly, in individual cases increased tracer uptake was already observed before contrast enhancement became apparent on MRI as part of the IRIS and before PML lesions became clearly visible on T2/FLAIR or DWI images. These initial observations indicate that TSPO PET might be able to detect PML lesions already during their formation phase – a finding that is consistent with the idea that local microglial cells rapidly sense and react to changes in the brain environment [37,38]. In this context it is interesting to note that TSPO uptake preceding MRI detection of contrast enhancement has also been reported for MS lesions [39]. Such early lesion detection would be of particular importance in a condition like natalizumab-associated PML, in which lesions likely start to form months before clinical symptoms become apparent [1,40] and early diagnosis and cessation of immunosuppression are critical for clinical outcome [41]. Frequent brain MRI scans are the most sensitive and clinically applicable imaging technique for early detection of suspect brain lesions in patients at risk of natalizumab-associated PML. However, a definite diagnosis of such suspect lesions based on MRI alone often remains challenging arguing for multi-modal imaging approaches that include techniques such as TSPO PET that assess defined pathological aspects of such lesions. In this context, it is interesting to note that a recent case report suggested that FDG PET can be used to differentiate hypometabolic PML lesions from hypermetabolic PML-IRIS lesions early in the course of natalizumab-associated PML [42]. Correspondingly 1H magnetic resonance spectroscopy (1H-MRS) has been shown to detect characteristic metabolic patterns in PML lesions that differentiate disease-stages during the course of PML in MS patients [43,44].

While tracer uptake reaches peak levels during the IRIS phase, we subsequently observed a slow decline of TSPO tracer uptake that however remained clearly elevated compared to intact brain tissue for the entire observation period of more than four years after PML diagnosis. This temporal profile is in marked contrast to the evolution of gadolinium enhancement that is only present in the IRIS stage and returns to baseline levels within few weeks thereafter. The

presence of TSPO tracer uptake along the entire course of PML raises the possibility that it can be used to stage inflammatory activity of PML lesions and thereby monitor progression of natalizumab-associated PML [45]. In addition TSPO-PET imaging may thus become useful to monitor treatment responses in natalizumab-associated and other PML cases, for example to new immunotherapies or anti-viral agents [45-47]. Furthermore the remarkably stereotypic decline of tracer uptake argues that in most patients with natalizumab-associated PML, inflammation resolves in a uniform and therefore predictable pattern.

The need to re-start MS therapies in patients with natalizumab-associated PML usually emerges when patients start to develop new clinical symptoms months to years after the initial PML symptoms [6,48]. In principle, these symptoms could be caused by a re-emergence of MS activity or a further progression of PML. Differentiating between these two scenarios is obviously critical as they lead to vastly different therapeutic consequences. MRI scans can provide important clues to facilitate this differentiation as a number of MRI features suggestive of PML lesions such as a subcortical location involving U-fibers, ill-defined borders towards white matter but sharp demarcation to the grey matter, T1w hypointensity, diffusion-weighted imaging hyperintensity and punctate T2w-hyperintensities with a relative lack of contrast enhancement have been described [1,49]. However, as no single feature is pathognomonic for PML, the differentiation from MS is challenging in particular when PML lesions are small [25] or when new MS lesions appear in the vicinity of a pre-existing PML lesion (see **Figure 5A**). As JCV may persist over a long period of time in the CSF or vice versa may be negative in some patients with ongoing PML, repeated CSF analysis alone may not be sufficient to differentiate MS disease activity from PML progression [1]. In these cases our study indicates that TSPO PET imaging can be helpful: first, because measuring tracer uptake in the pre-existing PML lesion allows to judge its lesional activity (in particular when compared to previous images or the decay curve described here) and second, because the TSPO-based diagnostic matrix we describe here can distinguish the vast majority of PML and MS lesions. We constructed this matrix based on three parameters that quantify distinct traits of maximal tracer uptake (SUVR[Max], lesion shape ("sphericity") and the signal texture within the lesion ("inertia"). The "sphericity" parameter makes use of the fact that most MS lesions appear round or ovoid [50], while PML lesion often show a more irregular shape [51]. While measuring maximal tracer uptake (SUVR[Max]) primarily relates the other parameters to the corresponding lesion activity, the "inertia" parameter leverages the micro-anatomy of PML lesions that compared to most active MS lesions are not confluent sites of increased inflammatory activity but rather clusters of multiple small inflammatory foci that can be readily detected in TSPO-imaging (c.f.

Figure 1A and **1B**, **Figure 3A** and **Supplementary Figure 1**). While this matrix allowed us to correctly assign most of the newly formed lesions observed in our study patients (**Figure 5**), one has to keep in mind that such discrimination might be more challenging for very small PML lesions (**Supplementary Figure 4**) or unusually large "tumefactive" MS lesions.

What can we learn from our results regarding the nature of the inflammatory reaction in natalizumab-associated PML? The stereotypic decline of inflammatory activity probably reflects the predictable clearance of the infection by the reconstituted and a priori competent immune systems of the affected patients. Yet, while inflammatory activity does decline over time, this process occurs slowly over the course of many months and PML lesions still show elevated tracer uptake at the longest observation points of our study 52 months after PML diagnosis. This is in stark contrast to tracer uptake in MS lesions that usually returns to baseline levels within 6 months after initiation of rituximab therapy (see **Figure 5C**). This indicates that in PML lesions major contributors to local innate immune responses such as phagocytes and astrocytes remain in an activated state for years after the initial formation of the PML lesion. This could merely be reflective of an ongoing local adaptive immune response but the emerging roles of innate immune cells in both regulating CNS inflammation and tissue remodeling [52,53] suggests a more active contribution to PML lesion fate that will be important to explore further.

Several limitations have to be considered when assessing our study and its conclusions. First, while a number of different radioligands for TSPO have been generated over recent years, none are without draw-backs [9,54]. In the case of the TSPO ligand [^{18}F] GE180 [30,55,24,20,56] we use here, the most prominent draw-back is that it shows a rather low brain penetration across the intact blood-brain-barrier (BBB) in humans [22]. Tracer uptake is therefore likely to be susceptible to alterations affecting BBB permeability [21,57,58]. Marked changes of BBB permeability, which can be visualized by gadolinium enhancement on MRI, can thus contribute to the enhanced tracer uptake observed during IRIS. However, they are unlikely to explain the substantial tracer uptake preceding contrast enhancement on MRI (as shown in **Figure 2**) or to underlie the long-lasting tracer accumulation in PML lesions that showed a more prolonged time-course than gadolinium enhancement (c.f. **Figure 3B** and **3C**). In contrast a contribution of putative "micro BBB damage", which would allow passage of the TSPO tracer but not of gadolinium is difficult to exclude based on our measurements. One should note however that a recent competitive binding study showed a comparably high specific binding of the [^{18}F] GE180 tracer in the brains of MS patients [59] and that our own histological analysis confirms that the spatial distribution of the TSPO target in brain sections from patients with natalizumab-associated PML matches the tracer signal observed in our study. The CNS inflammatory activity we measure here could thus

ultimately result from a combination of increased TSPO presence based on the infiltration of monocyte-derived macrophages as well as the activation of local microglial cells and enhanced tracer access based on micro-perturbations of the blood-brain barrier that result from this local inflammation. This might be one explanation why the density of TSPO-positive cells but not the TSPO uptake differ between MS and PML lesions (c.f. **Figure 1F** and **Supplementary Table 2**). Thus PET imaging approaches that can more directly assess aspects of blood-brain barrier function might be one approach to better untangle the relative contributions of target expression and target access to the observed tracer signals [60-62]

A second limitation of our study is that – as PML is a rare complication of natalizumab therapy – it is based on a small sample size of eight patients. Most of these patients were scanned repeatedly so that overall our analysis is derived from 16 TSPO PET scans. As TSPO PET imaging (not the least due to the local tracer synthesis) is a logistically demanding examination technique these numbers of scans are comparable to other recent (TSPO) PET imaging studies often conducted in more prevalent conditions [63,64]. Still, this is a pilot study performed at a single center and it will be important to validate the robustness of key parameters that describe the stereotypic decline of inflammatory lesion activity or define the TSPO-based diagnostic matrix in larger patient cohorts and across different PET scanner settings. This is in particular important for the TSPO-based diagnostic matrix that was developed based on a training set of highly active MS lesions (Unterrainer *et al*., 2018) and is thus geared towards the differentiation of Gd-enhancing MS lesions from PML lesions.

In conclusion we demonstrate that TSPO PET imaging can provide an approach to monitor inflammatory activity in patients with natalizumab-associated PML. Our histological analysis confirms the rationale for this approach by showing that TSPO-expressing cells, most of them mononuclear phagocytes, accumulate in early PML lesions. TSPO PET imaging in patients shows that inflammatory activity in PML lesions is more extensive than indicated on T2w-FLAIR and DWI and can be monitored throughout the disease course. Enhanced tracer uptake is present from the early stages of disease, peaks around immune reconstitution and subsequently follows a one-phase decay curve. The remarkable adherence of the patients in our study to this decay curve supports the notion that PML activity declines in a rather stereotypic and thus predictable manner after immune-reconstitution in patients with natalizumab-associated PML. Finally, a diagnostic matrix based on the intensity and morphometry of TSPO signals may be used to distinguish PML and MS lesions and help differentiating PML progression from MS re-occurrence.

Acknowledgements

We would like to thank Reinhard Hohlfeld for critical reading of the manuscript.

Funding

Work in M.Ke.'s laboratory is financed through grants from the Deutsche Forschungsgemeinschaft (DFG; including Transregio TRR128 and Transregio TRR274/1 2020-408885537), the European Research Council under the European Union's Seventh Framework Program (FP/2007-2013; ERC Grant Agreement n. 310932), the German Multiple Sclerosis Society and the "Verein Therapieforschung für MS-Kranke e.V." M.Ke. and T.K. are funded by the German Federal Ministry of Research and Education (BMBF) as members of the Clinical Competence Network Multiple Sclerosis, M.Ke. and P.B. are supported by the Munich Cluster for Systems Neurology (EXC 2145) and N.L.A. and P.B are supported by the DFG (research group FOR 2858). N.L.A. is supported by a research grant of the Else Kröner-Fresenius-Stiftung. Initial stages of the project were further supported by a research grant from Biogen to M.Ke. JH is funded by the German Federal Ministry of Education and Research (Grant Numbers 01ZZ1603[A-D] and 01ZZ1804[A-H] (DIFUTURE)).

Author Contributions

M.Ke., T.K., P.B., N.A., A-M.S. and C.M. conceived the experiments and performed statistical analysis. D.M., C.S., I.M. and W.B. provided tissue samples and performed histopathological analysis. T.K., M.M., J.H., M.Kr., A-M.S. and C.M. recruited and clinically characterized study patients. S.L. was responsible for radiopharmaceutical production. M.U., P.B. and N.A. were responsible for PET data acquisition. T.H. performed PET image reconstruction and processing. L.K. performed quantitative PET analysis V.M. performed analysis of binding affinity status. M.U., L. K., S.L., P.B. and N.A. acquired and analyzed PET and B.E.W., M.P., K.S., J.N. and A.G. acquired and assessed MRI data. M.Ke., T.K., A-M.S. and C.M. wrote the paper.

Competing interests

A.G. has received honoraria for lecturing, travel expenses for attending meetings, and financial support for research from Novartis, Biogen, Merck Serono, Sanofi-Genzyme, Roche. T.K. has received speaker and advisory board honoraria from Bayer Healthcare, Teva, Merck, Novartis,

Sanofi, Roche and Biogen as well as grant support from Novartis and Chugai Pharma. M.Ke. has been on advisory boards for Biogen, medDay Pharmaceuticals, Novartis and Sanofi, has received grant support from Sanofi and Biogen (including for the initial phase of this study) and speakers fees from Abbvie, Almirall, Biogen, medDay Pharmaceuticals, Merck Serono, Novartis, Roche, Sanofi and Teva. The rest of the authors report no disclosures related to this study.

References

1. Major EO, Yousry TA, Clifford DB. Pathogenesis of progressive multifocal leukoencephalopathy and risks associated with treatments for multiple sclerosis: a decade of lessons learned. *Lancet Neurol*. 2018;17(5):467-480. doi:10.1016/S1474-4422(18)30040-1

2. Biogen. *Biogen Safety Update 03/2020: Worldwide Postmarketing-Update for PML Under Natalizumab (Tysabri)*; 2020.

3. Hoepner R, Kolb EM, Dahlhaus S, et al. Predictors of severity and functional outcome in natalizumab-associated progressive multifocal leukoencephalopathy. *Mult Scler*. 2017;23(6):830-835. doi:10.1177/1352458516667241

4. Dong-Si T, Richman S, Wattjes MP, et al. Outcome and survival of asymptomatic PML in natalizumab-treated MS patients. *Ann Clin Transl Neurol*. 2014;1(10):755-764. doi:10.1002/acn3.114

5. Prosperini L, Kinkel RP, Miravalle AA, Iaffaldano P, Fantaccini S. Post-natalizumab disease reactivation in multiple sclerosis: systematic review and meta-analysis. *Ther. Adv. Neurol. Disord.* 2019;12:1756286419837809. doi:10.1177/1756286419837809

6. Maillart E, Vidal J-S, Brassat D, et al. Natalizumab-PML survivors with subsequent MS treatment: Clinico-radiologic outcome. *Neurol Neuroimmunol Neuroinflamm*. 2017;4(3):e346. doi:10.1212/NXI.0000000000000346

7. Igra MS, Paling D, Wattjes MP, Connolly DJA, Hoggard N. Multiple sclerosis update: use of MRI for early diagnosis, disease monitoring and assessment of treatment related complications. *Br. J. Radiol.* 2017;90(1074):20160721. doi:10.1259/bjr.20160721

8. Wijburg MT, Witte BI, Vennegoor A, et al. MRI criteria differentiating asymptomatic PML from new MS lesions during natalizumab pharmacovigilance. *J. Neurol. Neurosurg. Psychiatry*. 2016;87(10):1138-1145. doi:10.1136/jnnp-2016-313772

9. Matthews PM. Chronic inflammation in multiple sclerosis - seeing what was always there. *Nat Rev Neurol*. 2019;15(10):582-593. doi:10.1038/s41582-019-0240-y

10. Cosenza-Nashat M, Zhao M-L, Suh H-S, et al. Expression of the translocator protein of 18 kDa by microglia, macrophages and astrocytes based on immunohistochemical localization in abnormal human brain. *Neuropathol. Appl. Neurobiol.* 2009;35(3):306-328. doi:10.1111/j.1365-2990.2008.01006.x

11. Nutma E, Stephenson JA, Gorter RP, et al. A quantitative neuropathological assessment of translocator protein expression in multiple sclerosis. *Brain*. 2019;142(11):3440-3455. doi:10.1093/brain/awz287

12. Banati RB, Newcombe J, Gunn RN, et al. The peripheral benzodiazepine binding site in the brain in multiple sclerosis: quantitative in vivo imaging of microglia as a measure of disease activity. *Brain*. 2000;123 (Pt 11):2321-2337. doi:10.1093/brain/123.11.2321

13. Rissanen E, Tuisku J, Rokka J, et al. In Vivo Detection of Diffuse Inflammation in Secondary Progressive Multiple Sclerosis Using PET Imaging and the Radioligand ^{11}C-PK11195. *J Nucl Med*. 2014;55(6):939-944. doi:10.2967/jnumed.113.131698

14. Datta G, Colasanti A, Rabiner EA, et al. Neuroinflammation and its relationship to changes in brain volume and white matter lesions in multiple sclerosis. *Brain*. 2017;140(11):2927-2938. doi:10.1093/brain/awx228

15. Bodini B, Stankoff B. PET is necessary to make the next step forward in understanding MS pathophysiology - Yes. *Mult Scler*. 2019;25(8):1086-1087. doi:10.1177/1352458519828298

16. Yokokura M, Terada T, Bunai T, et al. Depiction of microglial activation in aging and dementia: Positron emission tomography with 11CDPA713 versus 11C(R)PK11195. *J Cereb Blood Flow Metab*. 2017;37(3):877-889. doi:10.1177/0271678X16646788

17. Mahler C, Unterrainer M, Muth C, et al. Imaging microglial activation in tacrolimus-associated CNS vasculitis with translocator protein PET. *Neurology*. 2018;91(20):936-937. doi:10.1212/WNL.0000000000006516

18. Metz I, Radue E-W, Oterino A, et al. Pathology of immune reconstitution inflammatory syndrome in multiple sclerosis with natalizumab-associated progressive multifocal leukoencephalopathy. *Acta Neuropathol*. 2012;123(2):235-245. doi:10.1007/s00401-011-0900-5

19. Moll NM, Rietsch AM, Ransohoff AJ, et al. Cortical demyelination in PML and MS: Similarities and differences. *Neurology*. 2008;70(5):336-343. doi:10.1212/01.WNL.0000284601.54436.e4

20. Unterrainer M, Mahler C, Vomacka L, et al. TSPO PET with [F]GE-180 sensitively detects focal neuroinflammation in patients with relapsing-remitting multiple sclerosis. *Eur. J. Nucl. Med. Mol. Imaging*. 2018;45(8):1423-1431. doi:10.1007/s00259-018-3974-7

21. Unterrainer M, Fleischmann DF, Vettermann F, et al. TSPO PET, tumour grading and molecular genetics in histologically verified glioma: a correlative 18F-GE-180 PET study. *Eur J Nucl Med Mol Imaging*. 2019. doi:10.1007/s00259-019-04491-5

22. Zanotti-Fregonara P, Pascual B, Rizzo G, et al. Head-to-Head Comparison of 11C-PBR28 and 18F-GE180 for Quantification of the Translocator Protein in the Human Brain. *J Nucl Med*. 2018;59(8):1260-1266. doi:10.2967/jnumed.117.203109

23. Berger JR, Aksamit AJ, Clifford DB, et al. PML diagnostic criteria: consensus statement from the AAN Neuroinfectious Disease Section. *Neurology*. 2013;80(15):1430-1438. doi:10.1212/WNL.0b013e31828c2fa1

24. Fan Z, Calsolaro V, Atkinson RA, et al. Flutriciclamide (18F-GE180) PET: First-in-Human PET Study of Novel Third-Generation In Vivo Marker of Human Translocator Protein. *J Nucl Med*. 2016;57(11):1753-1759. doi:10.2967/jnumed.115.169078

25. Yousry TA, Pelletier D, Cadavid D, et al. Magnetic resonance imaging pattern in natalizumab-associated progressive multifocal leukoencephalopathy. *Ann. Neurol.* 2012;72(5):779-787. doi:10.1002/ana.23676

26. Filippi M, Preziosa P, Banwell BL, et al. Assessment of lesions on magnetic resonance imaging in multiple sclerosis: practical guidelines. *Brain*. 2019;142(7):1858-1875. doi:10.1093/brain/awz144

27. Wickstrøm T, Clarke A, Gausemel I, et al. The development of an automated and GMP compliant FASTlab™ Synthesis of (18) FGE-180; a radiotracer for imaging translocator protein (TSPO). *J Labelled Comp Radiopharm*. 2014;57(1):42-48. doi:10.1002/jlcr.3112

28. Hammers A, Allom R, Koepp MJ, et al. Three-dimensional maximum probability atlas of the human brain, with particular reference to the temporal lobe. *Hum Brain Mapp*. 2003;19(4):224-247. doi:10.1002/hbm.10123

29. Gousias IS, Rueckert D, Heckemann RA, et al. Automatic segmentation of brain MRIs of 2-year-olds into 83 regions of interest. *Neuroimage*. 2008;40(2):672-684. doi:10.1016/j.neuroimage.2007.11.034

30. Vomacka L, Albert NL, Lindner S, et al. TSPO imaging using the novel PET ligand [F]GE-180: quantification approaches in patients with multiple sclerosis. *EJNMMI Res*. 2017;7(1):89. doi:10.1186/s13550-017-0340-x

31. Leijenaar RTH, Nalbantov G, Carvalho S, et al. The effect of SUV discretization in quantitative FDG-PET Radiomics: the need for standardized methodology in tumor texture analysis. *Sci. Rep.* 2015;5:11075. doi:10.1038/srep11075

32. Papp L, Rausch I, Grahovac M, Hacker M, Beyer T. Optimized Feature Extraction for Radiomics Analysis of 18F-FDG PET Imaging. *J Nucl Med*. 2019;60(6):864-872. doi:10.2967/jnumed.118.217612

33. Dickens AM, Vainio S, Marjamäki P, et al. Detection of microglial activation in an acute model of neuroinflammation using PET and radiotracers 11C-(R)-PK11195 and 18F-GE-180. *J. Nucl. Med.* 2014;55(3):466-472. doi:10.2967/jnumed.113.125625

34. Kaunzner UW, Kang Y, Zhang S, et al. Quantitative susceptibility mapping identifies inflammation in a subset of chronic multiple sclerosis lesions. *Brain*. 2019;142(1):133-145. doi:10.1093/brain/awy296

35. Coughlin JM, Yang T, Rebman AW, et al. Imaging glial activation in patients with post-treatment Lyme disease symptoms: a pilot study using 11CDPA-713 PET. *J Neuroinflammation*. 2018;15(1):346. doi:10.1186/s12974-018-1381-4

36. Wang Y, Coughlin JM, Ma S, et al. Neuroimaging of translocator protein in patients with systemic lupus erythematosus: a pilot study using 11CDPA-713 positron emission tomography. *Lupus*. 2017;26(2):170-178. doi:10.1177/0961203316657432

37. Kierdorf K, Prinz M. Microglia in steady state. *J. Clin. Invest.* 2017;127(9):3201-3209. doi:10.1172/JCI90602

38. Deczkowska A, Keren-Shaul H, Weiner A, Colonna M, Schwartz M, Amit I. Disease-Associated Microglia: A Universal Immune Sensor of Neurodegeneration. *Cell*. 2018;173(5):1073-1081. doi:10.1016/j.cell.2018.05.003

39. Oh U, Fujita M, Ikonomidou VN, et al. Translocator protein PET imaging for glial activation in multiple sclerosis. *J Neuroimmune Pharmacol*. 2011;6(3):354-361. doi:10.1007/s11481-010-9243-6

40. Lindå H, Heijne A von, Major EO, et al. Progressive multifocal leukoencephalopathy after natalizumab monotherapy. *N. Engl. J. Med.* 2009;361(11):1081-1087. doi:10.1056/NEJMoa0810316

41. Vermersch P, Kappos L, Gold R, et al. Clinical outcomes of natalizumab-associated progressive multifocal leukoencephalopathy. *Neurology*. 2011;76(20):1697-1704. doi:10.1212/WNL.0b013e31821a446b

42. Baheerathan A, McNamara C, Kalam S, et al. The utility of FDG-PET imaging in distinguishing PML-IRIS from PML in a patient treated with natalizumab. *Neurology*. 2018;91(12):572-573. doi:10.1212/WNL.0000000000006213

43. Schneider R, Bellenberg B, Hoepner R, Ellrichmann G, Gold R, Lukas C. Insight into Metabolic 1H-MRS Changes in Natalizumab Induced Progressive Multifocal Leukoencephalopathy Brain Lesions. *Front Neurol*. 2017;8:454. doi:10.3389/fneur.2017.00454.

44. Schneider R, Bellenberg B, Hoepner R, et al. Metabolic profiles by 1H-magnetic resonance spectroscopy in natalizumab-associated post-PML lesions of multiple sclerosis patients who survived progressive multifocal leukoencephalopathy (PML). *PLoS ONE*. 2017;12(4):e0176415. doi:10.1371/journal.pone.0176415.

45. Cortese I, Muranski P, Enose-Akahata Y, et al. Pembrolizumab Treatment for Progressive Multifocal Leukoencephalopathy. *N Engl J Med*. 2019;380(17):1597-1605. doi:10.1056/NEJMoa1815039

46. Küpper C, Heinrich J, Kamm K, Bücklein V, Rothenfusser S, Straube A. Pembrolizumab for progressive multifocal leukoencephalopathy due to primary immunodeficiency. *Neurol Neuroimmunol Neuroinflamm*. 2019;6(6):e628. doi:10.1212/NXI.0000000000000628

47. Mahler C, Andrews M, Henson SM, Gnanapavan S. Sequential interleukin 2 and pembrolizumab use in progressive multifocal leukoencephalopathy. *Neurol Neuroimmunol Neuroinflamm*. 2020;7(4). doi:10.1212/NXI.0000000000000756

48. Hoepner R, Faissner S, Ellrichmann G, Schneider R, Gold R. Rituximab postprogressive multifocal leukoencephalopathy: a Feasible therapeutic option in selected cases. *Ther. Adv. Neurol. Disord.* 2014;7(6):289-291. doi:10.1177/1756285614556287

49. Hodel J, Darchis C, Outteryck O, et al. Punctate pattern: A promising imaging marker for the diagnosis of natalizumab-associated PML. *Neurology*. 2016;86(16):1516-1523. doi:10.1212/WNL.0000000000002586

50. Rovira À, Barkhof F. Multiple Sclerosis and Variants. In: Barkhof F, Jager R, Thurnher M, Rovira Cañellas A, eds. *Clinical Neuroradiology*. Springer International Publishing; 2018:1-41.

51. Honce JM, Nagae L, Nyberg E. Neuroimaging of Natalizumab Complications in Multiple Sclerosis: PML and Other Associated Entities. *Mult. Scler. Int.* 2015;2015:809252. doi:10.1155/2015/809252

52. Prinz M, Jung S, Priller J. Microglia Biology: One Century of Evolving Concepts. *Cell*. 2019;179(2):292-311. doi:10.1016/j.cell.2019.08.053

53. Wheeler MA, Clark IC, Tjon EC, et al. MAFG-driven astrocytes promote CNS inflammation. *Nature*. 2020;578(7796):593-599. doi:10.1038/s41586-020-1999-0

54. Cumming P, Burgher B, Patkar O, et al. Sifting through the surfeit of neuroinflammation tracers. *J Cereb Blood Flow Metab*. 2018;38(2):204-224. doi:10.1177/0271678X17748786

55. Boutin H, Murray K, Pradillo J, et al. 18F-GE-180: a novel TSPO radiotracer compared to 11C-R-PK11195 in a preclinical model of stroke. *Eur. J. Nucl. Med. Mol. Imaging*. 2015;42(3):503-511. doi:10.1007/s00259-014-2939-8

56. Feeney C, Scott G, Raffel J, et al. Kinetic analysis of the translocator protein positron emission tomography ligand 18FGE-180 in the human brain. *Eur J Nucl Med Mol Imaging*. 2016;43(12):2201-2210. doi:10.1007/s00259-016-3444-z

57. Zanotti-Fregonara P, Veronese M, Pascual B, Rostomily RC, Turkheimer F, Masdeu JC. The validity of 18F-GE180 as a TSPO imaging agent. *Eur J Nucl Med Mol Imaging*. 2019;46(6):1205-1207. doi:10.1007/s00259-019-4268-4

58. Albert NL, Unterrainer M, Brendel M, et al. In response to: The validity of 18F-GE180 as a TSPO imaging agent. *Eur J Nucl Med Mol Imaging*. 2019;46(6):1208-1211. doi:10.1007/s00259-019-04294-8

59. Sridharan S, Raffel J, Nandoskar A, et al. Confirmation of Specific Binding of the 18-kDa Translocator Protein (TSPO) Radioligand [F]GE-180: a Blocking Study Using XBD173 in Multiple Sclerosis Normal Appearing White and Grey Matter. *Mol. Imaging Biol.* 2019. doi:10.1007/s11307-019-01323-8

60. Kreisl WC, Liow J-S, Kimura N, et al. P-glycoprotein function at the blood-brain barrier in humans can be quantified with the substrate radiotracer 11C-N-desmethyl-loperamide. *J Nucl Med*. 2010;51(4):559-566. doi:10.2967/jnumed.109.070151

61. Gerwien H, Hermann S, Zhang X, et al. Imaging matrix metalloproteinase activity in multiple sclerosis as a specific marker of leukocyte penetration of the blood-brain barrier. *Sci Transl Med*. 2016;8(364):364ra152. doi:10.1126/scitranslmed.aaf8020

62. Zoufal V, Mairinger S, Krohn M, et al. Measurement of cerebral ABCC1 transport activity in wild-type and APP/PS1-21 mice with positron emission tomography. *J Cereb Blood Flow Metab*. 2020;40(5):954-965. doi:10.1177/0271678X19854541

63. Sucksdorff M, Rissanen E, Tuisku J, et al. Evaluation of the Effect of Fingolimod Treatment on Microglial Activation Using Serial PET Imaging in Multiple Sclerosis. *J Nucl Med*. 2017;58(10):1646-1651. doi:10.2967/jnumed.116.183020

64. Dickstein LP, Liow J-S, Austermuehle A, et al. Neuroinflammation in neocortical epilepsy measured by PET imaging of translocator protein. *Epilepsia*. 2019;60(6):1248-1254. doi:10.1111/epi.15967

Figure legends

Figure 1: Activated mononuclear phagocytes show prominent TSPO expression in natalizumab-associated PML

(**A**): Immunostaining of brain autopsy tissue from a patient with confirmed natalizumab-associated PML (NTZ-PML) showing increased TSPO expression (TSPO: white) in the subcortical PML lesion area (left); heat-map representation of the TSPO immunosignal intensity reveals a reticular pattern of TSPO expression in PML lesions (right). (**B**) Immunostaining of brain biopsy tissue from a patient with a putative MS lesions (MS) showing strong TSPO expression (TSPO: white) in the lesional white matter (left); heat-map representation of spherical lesion (right). (**C**) Confocal images showing the different densities of TSPO-positive cells (TSPO: white, DAPI: blue) in NTZ-PML lesion white matter (left), lesion adjacent white matter (middle) and adjacent grey matter (right). (**D**) TSPO-positive cells (TSPO: white, DAPI: blue) in non natalizumab-associated PML (non MS PML) lesion white matter (left), putative multiple sclerosis lesion white matter (MS, middle) and non-inflamed control white matter (right). (**E**) Cell type-specific co-labeling indicates that TSPO is primarily expressed in CD68-positive phagocytes and GFAP-positive astrocytes in NTZ-PML (TSPO: white; DAPI: blue; GFAP: red; CD68: green); upper right: high magnification image of a TSPO-positive phagocyte; lower right: high magnification image of TSPO-positive astrocyte. (**F**) Quantitative analysis of the density of TSPO-positive cells in natalizumab-associated PML (NTZ-PML, n=4 patients), non natalizumab-associated PML (non MS PML, n=5 patients), putative multiple sclerosis lesions (MS, n=6 patients with clinically isolated syndrome/multiple sclerosis) and control white matter (n=4 cases). Three regions from each area were analysed, respectively. Fraction of the cellular identity of TSPO-positive cells, color-coded green (CD68+ phagocyte), red (GFAP+ astrocyte) and grey (CD68 and GFAP negative cells). $p < 0.05$ for NTZ-PML lesion WM, $p < 0.0001$ for Non MS PML and MS as compared to Control WM using 1-way ANOVA and post-hoc testing (Dunnett's multiple comparisons corrected). Only comparisons to Control WM are highlighted in the panel; when compared to MS lesion WM, all groups show a significant difference ($p < 0.0001$). Scale bars in **A**, 2000 μm; **B**, 200 μm; **C-D**, 50μm; **E**, 50 μm (left) and 10 μm (right).

Figure 2: Temporal evolution of MRI and TSPO PET presentation in Patient #3.

(A) Top row: T2-FLAIR. Center row: T2-FLAIR (PML lesion is colored in green to visualize lesion evolution). Bottom row: T1w after gadolinium. Below panel (A): Color bars indicate the phase of PML (red: PML before IRIS, orange: PML-IRIS, yellow: post-IRIS-PML). The PML lesion shows an increase in size up to the IRIS phase when prominent contrast enhancement is seen (white arrowhead). First signal abnormalities compatible with an emerging cortical PML lesion are seen at +3 (green arrowhead). A decrease in lesion size is observed after cessation of IRIS (months 8+9). **(B)** Corresponding TSPO PET, FLAIR and DWI at time points +3 and +9. (red and yellow arrow heads). At 3+: DWI hyperintensity marks acute PML lesion. Enhanced tracer uptake markedly exceeds the area of T2-FLAIR and DWI hyperintensity of the PML lesion. Contralaterally a cortical/subcortical patch of enhanced tracer uptake is also seen in the area of the putative new PML lesion. At +9 DWI isointensity and FLAIR regression demonstrate the typical phase of defect healing. At this point the TSPO PET lesion also shows decrease in size and tracer uptake intensity, that is still elevated compared to normal tissue. Lower right: Color reference bar indicating SUVR (0.0-4.0) in PET images.

Figure 3: TSPO PET imaging reveals stereotypic decline of TSPO tracer uptake in natalizumab-associated PML

(**A**) Appearance of PML lesions in MRI (upper row: T2/FLAIR; middle row: T1w with gadolinium) and TSPO PET imaging (lower row) at different time-points after diagnosis (top, months after diagnosis) in patients with natalizumab-associated PML (left #1, middle #4, right and far right #6). Lower right: Color reference bar for SUVR (0.0-4.0) in PET images. (**B**) Percentage of gadolinium positive voxels in T1w MRI within co-registered PET-derived lesion volumes of individual patients over time showed a short period of contrast enhancement in PML lesions (color-coded dots represent n = 8 patients at PET imaging timepoints, red circled dots show PML before IRIS, second timepoint contrast MRI of patient #4 was not acquired). Interpolated curves, starting at PML-IRIS stage, describe a one-phase decay with 95% confidence intervals. (C) TSPO-SUVR of the same PML lesions suggests a stereotypic decline of TSPO tracer uptake over time in natalizumab-related PML (color-coded dots represent n = 8 patients, red circled dots show PML before IRIS). Interpolated curves, starting at PML-IRIS stage, describe a one-phase decay with 95% confidence intervals.

Figure 4: Distinguishing PML and MS lesions using TSPO PET

(A) Illustration of MS- vs. PML-lesion morphology in TSPO PET scans reveals characteristic shape patterns (orange: MS lesion; green: PML lesion). (**B**) Differential clustering of MS- vs. PML lesions based on three-dimensional diagnostic matrix that combines quantitative imaging parameters of the uptake levels (SUVR[MAX]), as well as the shape (sphericity) and texture (inertia) of the uptake in TSPO PET, orange: n=89 MS lesions from n=17 MS-patients previously described by [20] green: n=23 PML lesion analyses (VOIs) from n=8 natalizumab-associated PML patients, ellipsoids show 95% confidence region (orange for MS lesions, green for PML lesions). (**C**) All lesions with high SUVR[MAX] (>2.9) can be clearly separated (grey: lesions with SUVR[MAX] <2.9, orange: MS lesions with SUVR[MAX] >2.9, green: PML lesions with SUVR[MAX] >2.9.

Figure 5: Effect of Rituximab treatment in post-IRIS-PML with recurrent MS activity

(**A**) Patient (#5) with recurrence of brain lesions in post-IRIS-PML before (left) and after rituximab treatment (right). Upper row: T2/FLAIR shows new lesions in the left cerebral peduncle and in the periventricular white matter. Middle row: T1w images show focal gadolinium uptake in several new lesions. Lower row: Tracer uptake in new lesions (orange circle) and the pre-existing PML lesion area. Reference bar for TSPO-SUVR on the right. (**B**) Quantitative analysis revealed MS-like features of the TSPO tracer uptake in 12 out of 13 (92%) new lesions (orange: n=13 lesions from four natalizumab-associated PML patients #5, #6, #7 and #8 with new brain lesions after PML) compared to PML lesions (green: n=7 PML lesion analyses from the same scan of the same patients: (#5, #6, #7 and #8,); 6 out of 7 PML lesion analyses (86%) were identified as PML by matrix analysis. Previously analysed PML and MS lesions from **Figure 4B** are shown in grey for comparison. Ellipsoids show 95% confidence region (orange for MS lesions, green for PML lesions, based on lesions analysed in **Figure 4B**. (**C**) Quantitative analysis of TSPO SUVR revealed differential tracer response to rituximab treatment of PML (left, mean of lesion analyses in patients #5, #6 and #7) compared to assigned MS-lesions (right, t0: pre rituximab treatment, t1: post rituximab treatment, patients #5, #6 and #7; for MS lesions $p<0.001$; no significant difference for mean TSPO SUVR for PML-lesions vs. MS-lesions at t0, t-test).

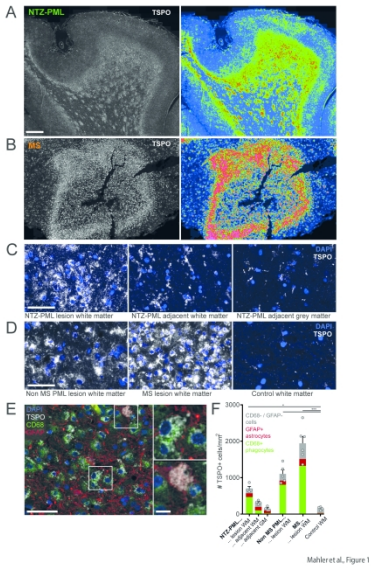

Figure 1

515x521mm (300 x 300 DPI)

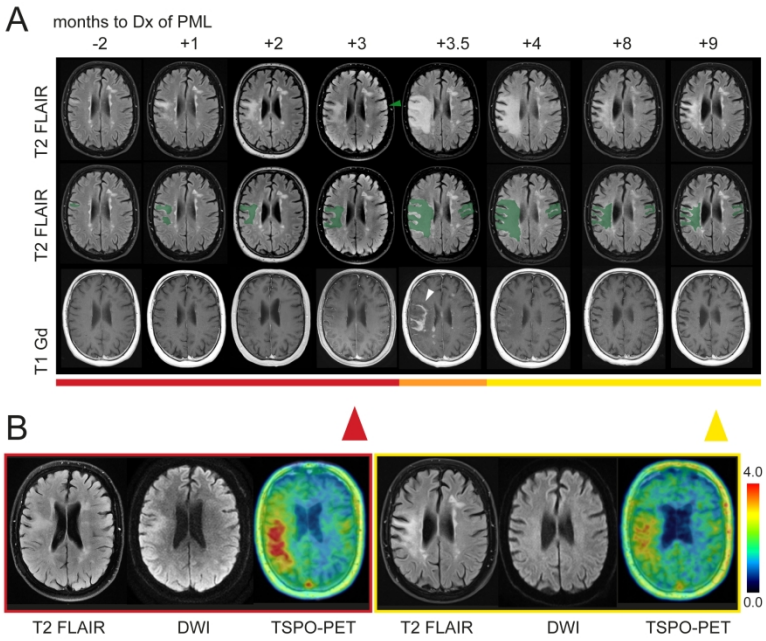

Mahler et al., Figure 2

Figure 2

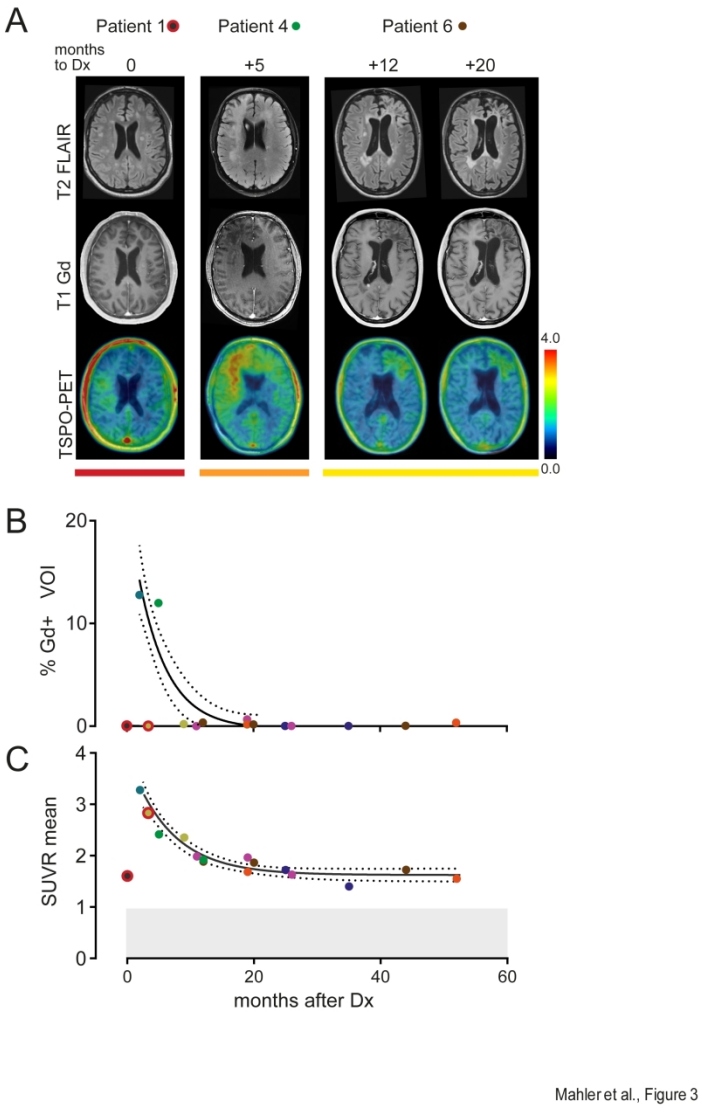

Mahler et al., Figure 3

Figure 3

210x297mm (300 x 300 DPI)

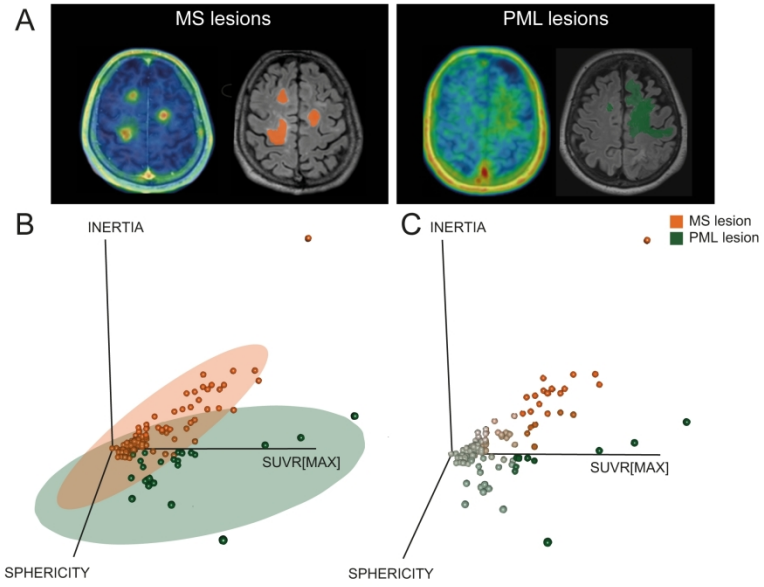

Mahler et al., Figure 4

Figure 4

210x297mm (300 x 300 DPI)

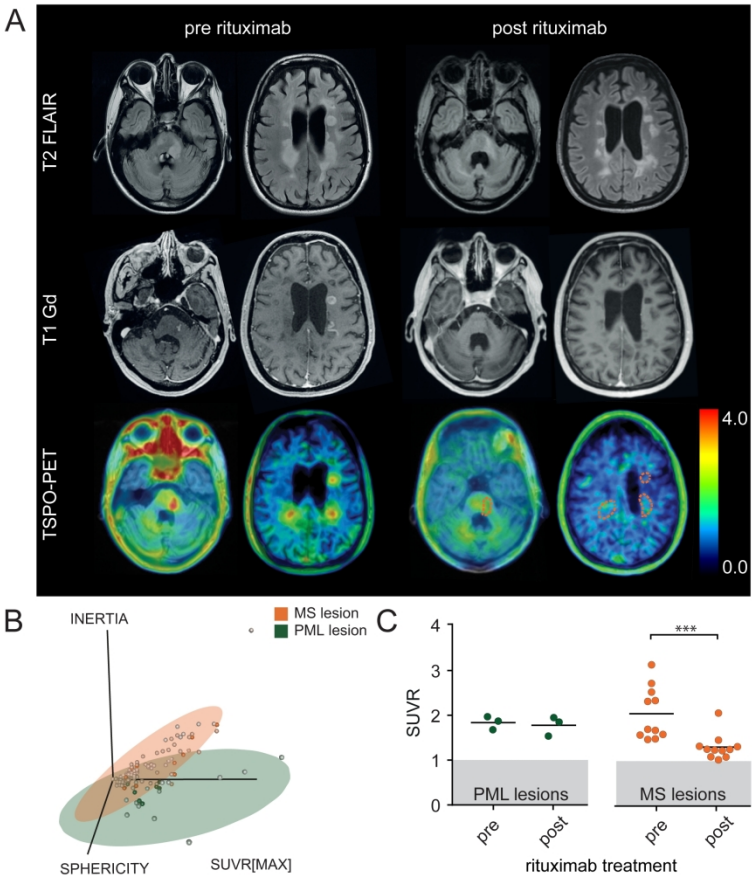

Mahler et al., Figure 5

Figure 5

222x286mm (300 x 300 DPI)

Table 1Demographic and clinical characteristics of natalizumab-associated PML cases included in the histopathological analysis

Pt no.	Sample	Age/Sex	NTZ infusions (n)	Last NTZ infusion to biopsy/autopsy (weeks)	First PML symptoms to biopsy/autopsy (months)	Clinical stage	PLEX/IA	JCV in CSF (copies/ml)
1	Autopsy	49/f	17	9	2	MS-PML	PLEX(2x), IA(3x)	Positive
2	Autopsy	60/m	40	14	2	MS-PML	PLEX(2x), IA(3x),	450000
3	Autopsy	40/m	58	13	3	MS-PML-IRIS	PLEX(5x)	112
4	Biopsy	25/f	27	14	3	MS-PML-IRIS	IA (5x),	Positive

NTZ = natalizumab; PML = progressive multifocal leukoencephalopathy; IRIS = immune reconstitution inflammatory syndrome; PLEX = plasma exchange; IA = immunoadsorption; JCV = polyomavirus JC; CSF = cerebrospinal fluid.

Table 2 Demographic and clinical characteristics of PML cases included in the PET imaging analysis

Pt no.	Age/Sex	EDSS	NTZ infusions (*n*)	last NTZ infusion to Dx of PML (w)	PET1 to Dx of PML (m)	PET2 to Dx of PML (m)	PET3 to Dx of PML (m)	PLEX/IA at Dx of PML	JCV in CSF at Dx of PML (copies/ml)	JCV-Ab index value in serum before Dx of PML	Clinical IRIS to Dx of PML (w)	Dx of PML to Rituximab(m)
1	40/m	4,0	71	15	0		-	-	2500	3.06	0	-
2	55/f	3.5	58	8	2	-	-	PLEX (2x)	309	2.36	6	-
3	51/m	4,5	79	3	3	9	-	-	44	1.08	17	-
4	56/m	3	48	0	5	12	-	IA (5x)	26	3.14	6	-
5	35/f	4	50	3	11	19	26	PLEX (7x)	30	3.55	5	12
6	40/f	4	46	0	12	20	44	PLEX (5x)	1440	3.70	7	14
7	37/m	4	52	2	19	52	-	IA (5x)	377	positive	6	20
8	50/f	6	66	6	25	35	-	PLEX (5x)	1300	0.81	5	45

EDSS = Extended disability status scale; NTZ = natalizumab; Dx = diagnosis; PML = progressive multifocal leukoencephalopathy; PLEX = plasma exchange; IA = immunoadsorption JCV = polyomavirus JC; CSF = cerebrospinal fluid; IRIS = immune reconstitution inflammatory syndrome; w = weeks; m = months; JCV-Ab index value data from Unilabs.